NATIONAL ADVISORY COMMITTEE FOR AERONAUTICS

TECHNICAL NOTE 2003

INVESTIGATION OF A NACA HIGH-SPEED STRAIN-GAGE TORQUEMETER

By John J. Rebeske, Jr.

Lewis Flight Propulsion Laboratory
Cleveland, Ohio

Washington
January 1950

NATIONAL ADVISORY COMMITTEE FOR AERONAUTICS

TN 2003

INVESTIGATION OF A NACA HIGH-SPEED STRAIN-GAGE TORQUEMETER

By John J. Rebeske, Jr.

SUMMARY

A strain-gage torquemeter employing a circuit to minimize effects of contact resistance was constructed and the performance under static and dynamic conditions was investigated.

Dynamic tests of this instrument were made over a range of shaft speed from 5000 to 17,000 rpm and torque loads from 250 to 5500 inch-pounds with corresponding torsion shaft stresses of 600 to 14,200 pounds per square inch. Effects of temperature, axial stress, slip-ring contact resistance, and speed on the operation of the torquemeter were investigated. Results of static calibration of the instrument over a range of torque and temperature and the magnitude of the effects of axial stress and slip-ring contact resistance on the static calibration are presented.

Repeated calibrations over 6 months indicated no change in the calibration constants. Dynamic operation over the range of speed and torque indicated an over-all probable accuracy and precision of ±0.33 percent of full-scale reading. This torquemeter was capable of sustained operation at speeds from 13,600 to 17,000 rpm for about 5 hours without requiring adjustment of brush-contact pressures.

It is recommended that for optimum accuracy, high torsion-shaft stress be employed and the torquemeter installation be free of axial stress.

INTRODUCTION

In basic compressor and turbine research where small accumulative gains in efficiency and performance must be measured, an accurate measurement of shaft power becomes extremely important. In order to meet this requirement, accuracies of the order of ±0.5 percent at shaft speeds up to 17,000 rpm are necessary. Because of the large equipment, it is frequently impracticable to cradle the equipment so that torque may be measured by determining the reaction

of the driving unit. The problem becomes even more complex at high speeds where shaft-speed ratios other than unity are required. The inherent losses in shaft-speed-ratio devices are difficult to measure accurately. A torque-measuring instrument capable of operation at high shaft speeds, which is simple, accurate, and dependable, is therefore most desirable.

In general, current torque-measuring instruments may be classified according to the following types: the torque-reaction type, the angular-twist type, and the surface-strain type.

The torque-reaction type makes use of Newton's third law and requires the measurement of some external reaction force. This type has the disadvantage of either cradling the power source or sink, or resorting to complicated gearing systems with their inherent losses in order to measure the reaction.

The angular-twist type utilizes the familiar principle of measuring the angular deflection in a gage length of shaft; the angular deflection is proportional to torque transmitted. The angle may be measured in a number of ways, but usually involves the mounting of complex precision assemblies directly on the rotating shaft.

The principle involved in the operation of the surface-strain type is the proportionality that exists between shaft torque and shaft-surface strain. Surface strain is measured by several methods, the most common of which uses electric strain gages cemented to the shaft surface. A typical example of this method is discussed in reference 1. When this method is used there are two principal difficulties to overcome: the effects of slip-ring contact resistance and the effects of temperature on the torsion shaft and the strain gages.

The surface-strain type and, in particular, the strain-gage method of measuring surface strain appears to offer the best possibility for meeting the needs of basic compressor and turbine research. Consequently, an investigation was undertaken at the NACA Lewis laboratory to determine by actual experiment if such an instrument could be developed that would be suited for practical use for basic compressor and turbine research within the necessary limits of speed, accuracy, and precision.

Such a strain-gage torquemeter was designed and built and the performance evaluated. An electric circuit was used that minimizes the effects of slip-ring contact resistance and permits the use of a potentiometer as an indicating instrument. A method is evolved to

evaluate and to correct for the effects of temperature on the torquemeter. Results of the performance investigations are presented for a range of shaft speed and torque loads from 5000 to 17,000 rpm and 250 to 5500 inch-pounds, respectively. Precision and accuracy is experimentally determined and expressed in terms of a probable deviation. Operating torsion-shaft stresses for maximum precision and accuracy are recommended and the dynamic operation of the instrument is discussed.

APPARATUS

Torquemeter

The strain-gage torquemeter consists of three basic parts: the torsion shaft, the slip rings, and a self-balancing potentiometer. The torsion shaft and the slip-ring assemblies are shown in figure 1.

Torsion shaft. - The hollow torsion shaft is fabricated from SAE 4140 steel, heat-treated to a Rockwell C hardness of 26 to 32. It is 17.8 inches long with a 2.0-inch test section. The inside and outside diameters of the test section are 1.000 and 1.391 inches, respectively. Spherical spline couplings are doweled and bolted to the ends of the torsion shaft. Four advance wire strain gages connected in the form of a Wheatstone bridge are bonded with bakelite cement to the outside surface of the test section. (See detail in figs. 1 and 2.) Wires from the bridge pass inwardly through holes drilled in the shaft a short distance away from the test section and are connected to a multiple-pronged plug, which is locked in place on the inside of the torsion shaft. Provision is made to complete electric connections to the plug after the torsion shaft is installed.

Slip rings and brushes. - The slip rings (fig. 3) consist of seven monel washers having an axial width of 0.187 inch and an overall diameter of 1.88 inches. These monel rings are assembled with bakelite insulating washers in a laminated fashion on a hollow shaft over which a bakelite sleeve has been placed. The circumferential surfaces of the monel rings are ground, after assembly, as smooth as possible to a concentricity of ±0.0002 inch. The shaft is mounted in oil-filled sintered bearings with provision for additional oiling, scavenging, and temperature measurement. The brushes, made of a mixture of 60-percent silver and 40-percent graphite, have a diameter of 0.125 inch and a length of 0.625 inch. Two brushes spaced 180° apart make electric contact with each of the slip rings. Each bank of brushes is positioned by a bakelite support (fig. 4), and individual brush pressure is obtained by means

of leaf springs 3 inches long made of Swedish spring steel. The thickness of the springs on one support is 0.008 inch and on the other 0.010 inch. Different spring thicknesses are employed to obtain different natural vibrational frequencies of the springs. This procedure assures uninterrupted electric contact with the slip rings should one set of brushes become inoperative because of induced critical vibration of the brush springs. Brush pressures are set by movement of the brush support using the support adjusting screws shown in figure 3.

Indicating instrument. - Torque values are indicated on a commercially available, self-balancing potentiometer, which was modified to include a circuit (reference 2) that minimizes the effects of small contact resistances between the brushes and the slip rings. The accuracy of the potentiometer when used in this manner is approximately ±0.2 percent.

Principle of operation. - A schematic diagram of the complete torquemeter circuit is shown in figure 5. The circuit design is based on the theory presented in reference 2. Four advance wire strain gages, which comprise the elements of the Wheatstone bridge, are bonded to the torsion shaft along 45° helices. When torque is applied to the test section, one pair of strain gages (opposite resistances in the bridge) lie on a path of maximum tensile stress; the remaining pair lie on a path of maximum compressive stress. The bridge circuit is thus sensitive to torsional stresses and relatively insensitive to axial and bending stresses. The diagonal corners of the bridge are supplied with 12-volt alternating current through slip rings A,B and C,D. Any unbalanced voltage is fed to the amplifier through slip rings, E, F, and G. This voltage is amplified and energizes a positioning motor (not shown), which drives the contact on the slide-wire S to a new position so that balance is again restored to the bridge. The position of the contact on the slide wire is indicated by a linear millivolt scale graduated from 0 to 10 millivolts in divisions of 0.02 millivolt. The helical potentiometer is used to adjust the zero on the millivolt scale. The resistances in the bridge supply circuit minimize the effect of small contact resistance.

Experimental Setup and Methods

The general experimental program consisted of static calibration of the torquemeter, dynamic operation of the instrument over a range of speed and load, and a comparison of the resulting dynamic torque values (based on the static calibrations) with a suitable standard, which consisted of a carefully calibrated dynamometer.

For the dynamic operation of the torquemeter, a 3000-horsepower variable-speed motor together with a speed-increasing gearbox was used as a power source. Power thus generated was transmitted through the torsion shaft and absorbed by the dynamometer. Simultaneous values of torque were indicated by the torquemeter and the dynamometer reaction.

Dynamometer Calibration

An eddy-current-absorption dynamometer rated at 1700 horsepower at a speed of 25,000 rpm was fitted with a torque cell to measure its reaction. A 63.00-inch moment arm fitted with a viscous vibration damper was provided for static loading. Dynamic loading was controlled by changing the field current. Heat generated in the stator was removed by circulating water through a stator jacket. The temperature of the cooling water emerging from the stator jacket was held at $120 \pm 20^{\circ}$ F.

The torque cell was capable of measuring the dynamometer reaction within ±0.1 percent (for any particular calibration) from reaction loads of 50 to 300 pounds. Dynamometer reaction loads were indicated on a 130-inch manometer; acetylene tetrabromide was used as the manometer fluid. Surge tanks were provided to reduce pressure fluctuations in the manometer line.

For accurate calibration, reducing the rotative stator movement to a minimum is desirable. The maximum movement of the load piston was approximately 0.0002 inch.

The dynamometer in the process of a static calibration is shown in figure 6. Calibration was accomplished by placing weights on the loading pan, which was suspended from the static-moment arm. The reaction to this applied torque, as indicated on the 130-inch manometer, was recorded for both increasing and decreasing torques from 0 to 6300 inch-pounds in increments of 315 inch-pounds. The average manometer-fluid temperature was also recorded.

Special precautions were taken to insure accurate and representative dynamometer calibrations. The dynamometer rotor shaft was uncoupled from the drive shaft to eliminate any hysteresis caused by the drive-shaft high-speed bearing friction. Water and oil hose connections to the stator were oriented to minimize any torque application to the dynamometer by forces transmitted through these connections. During static calibration, care was taken to duplicate, wherever possible, dynamic operating conditions. Similar

dynamometer oil and water pressures were maintained and the discharge temperature of the dynamometer cooling water was held near the average value observed during dynamic operation.

Manometer readings were corrected for the effects of temperature on the density of the acetylene tetrabromide. All manometer readings were corrected to a basic temperature of 50° F. These readings were then plotted against dynamometer torque.

Inasmuch as the dynamometer static calibrations were essentially linear, they were expressed in the form of a slope-intercept equation. The method of least squares was employed to determine the particular values of slope and intercept that most closely fitted the observed calibration data.

The equation was of the form

$$Y = MX + B \qquad (1)$$

where

Y corrected manometer reading, inches acetylene tetrabromide

M and B constants for a particular calibration

X torque, inch-pounds

The difference between measured torque values and torque values calculated from equation (1) is presented in figure 7 for a typical static calibration. The difference, or error, in inch-pounds is plotted against applied torque for both increasing and decreasing torque loads. The average value of the error for any given torque load is within ±0.1 percent of full load. The probable error of any one observed static reading for the aggregate of the calibrations was approximately ±0.05 percent of full load. Because of a variation in the dynamometer static calibration with time, however, the calibration was repeated at periodic intervals during the course of torquemeter dynamic operating studies.

In order to determine operating vibrational effects on the static calibration, an unbalanced air turbine was bolted to the static moment arm. A constant static torque was applied while the arm was vibrated through a range of frequencies corresponding to those observed through the limits of operating speeds, 5000 to 17,000 rpm. No measurable change

in the manometer reading was observed. The conclusion was therefore reached that the static calibrations were valid for dynamic operation.

Torsion-Shaft Static Calibration

Before using the torquemeter, static calibrations of the instrument must be obtained. This static calibration is accomplished by means of an apparatus consisting of two pedestals, a ball-type bearing, a 60.00-inch moment arm, and suitable calibration weights.

The torsion-shaft static calibration setup is shown in figure 8. A thin steel ribbon, which makes contact with the surface of the moment-arm arc at a constant radius of 60.00 inches, is used to attach the loading pan to the static-moment arm. The moment arm with the loading and counterbalance pans attached was balanced and keyed to one end of the torsion shaft. The torsion shaft was then mounted between two pedestals. One end of the shaft was supported by a ball bearing located on the rear pedestal, the other end was rigidly keyed to the front pedestal. After mounting, the moment arm and the torsion shaft were adjusted to a horizontal position and the moment arm set perpendicular to the axis of the torsion shaft. Electric connections were made to the bridge and thermocouples were mounted on the test section of the torsion shaft. In order to control the torsion-shaft temperature during calibration, an insulating box (not shown) was placed around the shaft. Temperatures higher than ambient were produced by placing heating elements inside this box. Temperatures lower than ambient were obtained by use of solid carbon dioxide. In this manner, shaft temperatures from 0° to 218° F could be established and maintained with temperature differentials at any point in the test section of the torsion shaft of not more than 2° F. Each of the calibration weights was 5 ± 0.004 pounds. Static calibrations were made over a range of shaft temperatures from 0° to 218° F by placing weights on the loading pan and recording the potentiometer readings corresponding to this known torque. Readings were thus recorded for both increasing and decreasing torque from 0 to 6300 inch-pounds. Calibrations were made with no contact resistance and again with simulated values of contact resistance in the circuit.

With zero torque in the torsion shaft, axial tensile forces were applied to the shaft in order to determine qualitatively the effects of axial tensile stress on the operation of the torquemeter. The torsion shaft was placed in a loading machine and tensile forces applied through ball-type connectors coated with high-pressure lubricant. In this manner, bending or torsion in the test section was avoided. After several loading cycles over a range of tensile stress from 0 to 30,000 pounds per square inch, the shaft was stressed in

increments of 1000 pounds per square inch and the change in the "zero" potentiometer reading was observed for both increasing and decreasing axial loads.

Dynamic Operation

For dynamic operation, the torsion shaft was coupled between the high-speed pinion drive shaft of the gearbox and the dynamometer as shown in figure 9(a). Coupling was made through spherical-type splines and sufficient axial clearance was provided in the couplings to prevent axial stresses in the torsion shaft. A shield with provisions for lubricating and scavenging the coupling splines was placed around the torsion-shaft assembly. An indication of torsion-shaft operating temperature was obtained by mounting a thermocouple inside the shield. The thermocouple bead was located opposite the strain gages at a radial distance of 1/4 inch from the test-section surface. Wires making electric connections to the multiple-pronged plug in the torsion shaft were passed through the hollow high-speed pinion drive shaft and the slip-ring drive shaft to the slip rings. A view of the slip-ring assembly installed at the rear of the gearbox is shown in figure 9(b).

Dynamic runs were made over a range of speeds from 5000 to 17,000 rpm in nominal steps of 1000 rpm. Critical dynamometer vibration prevented sustained operation from 11,000 to 13,500 rpm. Torque loads from 250 to 5500 inch-pounds were set in nominal increments of 1000 inch-pounds over the full range of speed. Runs were made by maintaining constant speed for both increasing and decreasing torque loads. Simultaneous readings of the torquemeter potentiometer and the dynamometer reaction manometer with torsion-shaft temperature, slip-ring contact resistance, and average manometer-fluid temperature were observed during these runs.

RESULTS AND DISCUSSION

The over-all evaluation of an instrument is based on the qualities, accuracy, precision, and practicability. Accuracy is defined by the order of agreement between the magnitude of a quantity as indicated by the instrument with the true magnitude. The precision is determined by its ability to repeat a reading under a given set of conditions. The practicability is judged by the efficiency (in terms of reliability, simplicity, convenience, and safety) with which it may be used to achieve the purpose for which it was designed. The static and dynamic performance of this torquemeter are evaluated on the basis of these qualities.

Torsion-Shaft Static Calibration

Because the strain-gage torquemeter indicates a quantity proportional to torque rather than torque itself, a suitable factor of proportionality must be obtained. Such a determination is achieved by static calibration. For static calibrations, accuracy was considered to be the order of agreement between any observation with the corresponding true value as established by applying the method of least squares to all the observations.

A typical static calibration of the torquemeter, at a torsion-shaft temperature of 73° F, is presented in figure 10 where potentiometer reading (mv) is plotted against shaft torque (in.-lb). Because of the limitations of the dynamic experimental equipment, torque values in static calibrations were restricted to 6300 inch-pounds. Similar static calibrations, repeated at intervals over 6 months yielded no evidence that the calibration was subject to drifting either with time or usage. Hysteresis is low, the average hysteresis value being less than 0.2 percent of full-scale reading. The plot of the observed points closely approaches a straight line. Accordingly, a linear relation between potentiometer reading and shaft torque was assumed in the form

$$y = mx + b \tag{2}$$

where

y potentiometer reading, millivolts

m slope of line, millivolts per inch-pound

x applied torque, inch-pound

b value of y at zero torque (intercept)

The method of least squares was employed to determine the particular values of m and b that made equation (2) most nearly fit the observed data. The probable error of any one observed reading from the true value, as determined by the equation corresponding to that calibration, was found to be ±0.08 percent of full-scale deflection.

Calibrations performed at various torsion-shaft temperatures differed; therefore values of m and b required to fit equation (2) to the observed data were calculated. These values, plotted against torsion-shaft temperature, are presented in figure 11. The variation

of slope with torsion-shaft temperature (fig. 11(b)) can be partly explained by the decrease in the torsional modulus of elasticity of the shaft (which can be shown to be inversely proportional to the slope) with increasing temperature. Information on this phenomenon is given in references 3 to 5. Calculations based on the following equation, (reference 3, p. 31) show a decrease in the torsional modulus of this shaft of 0.6 percent for a temperature rise of 50° F:

$$\frac{G}{G_0} = 1 - \left(\frac{T}{T_m}\right)^{\frac{2}{}}$$

where

G torsional modulus to be determined

G_0 torsional modulus at 0° R

T temperature at which G is desired, °R

T_m melting point of material, °R

This decrease is only indicative of the order of magnitude and is not considered a quantitative value. The value of 0.6 percent accounts for two-thirds of the actual observed decrease in torsional modulus. The remaining one-third is attributed to thermal-resistive and thermal-expansive properties of the strain gages.

Change in the intercept, the zero balance point of the bridge circuit, with temperature is attributed to small errors in mounting the strain gages on the true 45° helices and to the variance in the characteristics of the individual gages comprising the bridge. These factors cause a shift of the balance point of the bridge with temperature change. Both theory and experiment show this variation to be linear.

Because the torsion-shaft temperature is an independent variable affecting the static-calibration constants, shaft temperature must be obtained with an accuracy of ±5° F. Although the method used for determining the shaft temperature in this investigation was satisfactory, the mounting of a thermocouple directly on the torsion shaft is recommended.

When slip-ring contact resistance was simulated in the circuit, a decrease in the slopes of the static-calibration lines occured. No measurable effect on the intercepts existed. During dynamic

operation, the series resistance per pair of slip rings remained between 3 and 5 ohms. For static calibration, simulated contact resistances based on the 5-ohm value were inserted in the electric circuit. The extent to which contact resistance affects the slope is shown in figure 11(b). At a torsion-shaft temperature of 73° F, the slope is reduced by 0.5 percent when operating contact resistance is simulated.

Subsequent experimental investigation of the bridge circuit revealed that all first-order effects of contact resistance could be eliminated by omitting the connection between O and N (fig. 5) thus eliminating the need for experimentally determining the quantitive effect and the subsequent correction for it.

When the torsion-shaft temperature is known, corresponding values of slope and intercept are obtained from figure 11 and used in equation (2) to calculate shaft torque for a given potentiometer reading.

Axial-Stress Effects

In some installations, a torquemeter may be subjected to axial as well as torsional loads. Although axial-stress effects are compensated by employing a bridge-type circuit and by similar orientation of the strain gages on the shaft; full compensation may not be achieved because of dissimilarity in the characteristics of individual gages with inaccuracies in the orientation. Consequently, the torsion shaft was subjected to axial tensile loads to determine the resulting changes in the potentiometer zero readings. The potentiometer zero reading decreased 0.14 percent of full scale per 1000 pounds per square inch of tensile stress over a range from 0 to 30,000 pounds per square inch. On the basis of these findings, it is recommended that for optimum accuracy the torquemeter installation be such as to avoid axial stresses in the torsion shaft.

Dynamic Operation

The concept of instrument accuracy is extended to the dynamic performance in figure 12 where typical torquemeter operating data are presented for an average torsion-shaft temperature of 98° F and nominal torsion-shaft speed of 10,000 rpm. Torquemeter potentiometer reading is plotted against shaft torque, as indicated by the dynamometer reaction measurements. The maximum torque loading for this run was slightly greater than 5500 inch-pounds, which

represented the peak loading possible with the dynamic test equipment used. The static calibration for a torsion-shaft temperature of 98° F is represented by the dashed line in figure 12.

When dynamometer torque is considered to be representative of the true value, as was done for this investigation, the instrument retains a high degree of accuracy under operating conditions. For this representative run, the maximum deviation from static performance was 30 inch-pounds. In terms of instrument full-scale readings, this value represents a deviation of only 0.5 percent.

The torquemeter precision, as indicated by the ability to repeat readings, is shown in figure 13. Simultaneous values of dynamic shaft torque were indicated by the torquemeter and the dynamometer. Dynamic shaft torque indicated by the torquemeter was calculated from equation (2), which is based on static calibration, by using the observed potentiometer reading and the average torsion-shaft temperature. Dynamic shaft torque indicated by the dynamometer was calculated from equation (1) using observed manometer readings corrected for temperature with appropriate dynamometer static-calibration constants. Dynamometer torque was assumed to be the true torque value and was used as a basis for determining the accuracy of the torquemeter under dynamic conditions. The difference between these simultaneous values of shaft torque is called torquemeter deviation. This deviation in inch-pounds is plotted against dynamoeter torque values for a range of shaft speed from 5000 to 17,000 rpm.

The probable torquemeter deviation of any individual reading, based on the aggregate of data points, is ±20 inch-pounds or ±0.33 percent of full scale. Because the line of zero torquemeter deviation is collinear with the line corresponding to the assumed true torque value, the probable torquemeter deviation further represents the order of agreement between true (assumed) and indicated magnitudes and fixes the over-all instrument accuracy. The probable accuracy of any individual reading is thus set at ±0.33 percent of full scale. These values of precision and accuracy are within the desired limits, which were fixed at the beginning of this investigation.

The absence of any significant trends with speed throughout the range of operation is to be noted in figure 13. Such absence is noteworthy because it shows speed and centrifugal effects to be negligible within the experimental limits. The increased data scatter in the range of torque at and below 1000 inch-pounds is probably due to poor torque regulation of the power source at low torque loads. In this range of torque, the potentiometer scale was observed

to oscillate with an amplitude on the order of ±0.10 millivolt; whereas during operation at torque loads above 1000 inch-pounds, the amplitude reduced to a steady value of ±0.02 millivolt. In contrast, dynamometer speed and reaction readings were steady regardless of torque load because of the high degree of damping present in the dynamometer reaction-measuring system. The torquemeter, rather than the dynamometer, therefore indicates any small fluctuation in the torque load.

The minimum and maximum values of shearing stress (outer-surface fiber stress) during dynamic operation were approximately 600 and 14,200 pounds per square inch, respectively. The maximum allowable shearing stress for the material used in this shaft is on the order of 60,000 pounds per square inch. In the region of working stresses over which the torquemeter was operated, the investigation objectives of precision and accuracy were attained.

By raising the value of shaft working stress, however, the accuracy of the instrument will be increased by virtue of the corresponding increase in the ratio of signal voltage to extraneous signal voltage. With the type of electric circuit used, the extraneous signal voltage is relatively constant and is due primarily to contact resistance and the ratio of the unsteady component of torque to the steady component of torque.

High shaft-working stresses are therefore recommended with the maximum values limited by mechanical safety of the particular system. In order to obtain high shaft-working stress over a wide range of load, construction of more than one torsion shaft may be necessary, where each shaft is designed to operate over only a portion of the load range.

Operation of the slip rings at maximum rubbing-surface velocities of 140 feet per second presented a difficult problem. The smoothness and the concentricity of the individual slip-ring contact surfaces were critical. The requirements for satisfactory slip-ring operation were found to be 5 to 7 root mean square microinches for surface smoothness and ±0.0002 inch for the concentricity. These requirements may be somewhat relaxed if higher brush pressures are employed; however, high brush pressures will reduce the useful life of the brushes themselves. Brush pressures used were approximately 20 to 40 pounds per square inch. It is further imperative that no oil nor dirt particles be permitted to come in contact with the slip-ring surfaces or brushes. Even small deposits are sufficient to cause contamination.

Satisfactory performance was achieved with the dual-suspension-spring system. Uninterrupted slip-ring contact was obtained under all operating conditions.

Although this slip-ring configuration is subject to further improvements, continuous operation at rubbing-surface velocities from 112 to 140 feet per second (corresponding to shaft speeds of 13,600 and 17,000 rpm) for periods of about 5 hours was attained without requiring adjustment. During these periods of operation, the series resistance per pair of slip rings did not exceed the 5-ohm operating limit.

A necessary condition for accurate torque measurement by means of this torquemeter was that the minimum resistance to ground of the strain-gage bridge and slip rings be 45 megohms with the potentiometer out of the circuit. When the resistance to ground decreased to a lower value, the potentiometer reading does not indicate the true shaft torque. In several runs at high rotative speeds (with a correspondingly high slip-ring temperature) or at a high torsion-shaft temperature, the resistance to ground decreased below 45 megohms, resulting in an error in the torquemeter reading. This decrease was caused by a partial breakdown of the bakelite insulation of the slip rings and of the strain gages at temperatures above 200° F. Baking the slip-ring assembly and torsion shaft at approximately 250° F until the resistances were restored to the minimum value overcame this difficulty and satisfactory insulating properties at temperatures up to 250° F were obtained.

The investigation has demonstrated the feasibility of producing a reliable torque-measuring instrument capable of continuous operation over reasonable periods of time. This instrument has the characteristics of precision and accuracy required for use in current compressor and turbine research. Although the instrument is subject to additional refinements, it is, in the current form, relatively simple in structure and may be constructed at low cost. The strain gages and the basic potentiometer are commercially available. Instrument reliability has been proven by repeated calibration and operation over 6 months without indication of change in the static-calibration constants. Static-calibration characteristics are closely maintained during dynamic operation, eliminating the necessity of costly and time-consuming dynamic calibration. The design further permits remote reading of bridge-unbalance voltage with no loss in accuracy, a desirable safety feature when application is made to high-speed equipment operating at elevated temperature levels.

CONCLUDING REMARKS

From an investigation involving the study of a strain-gage torquemeter, the following results, conclusions, and recommendations were obtained:

1. A strain-gage torquemeter was developed that incorporates an electric circuit that minimizes effects of contact resistance and allows the use of a potentiometer as an indicating device. A practical method was evolved, which corrects for temperature effects on the torquemeter operation.

2. This torquemeter was operated over a range of speed from 5000 to 17,000 rpm and torque loads from 250 to 5500 inch-pounds with a probable accuracy and precision based on the aggregate of data points of ±0.33 percent of full-scale deflection. Continuous operation at speeds from 13,600 to 17,000 rpm for periods of about 5 hours was obtained without adjustment of brush contact pressures.

3. The reliability of this instrument was checked by repeated calibration and operation over 6 months; no change in the static-calibration constants was observed. The absence of any significant performance trends with speed through the range of operation showed that speed and centrifugal effects were negligible within the experimental limits. Because static calibration characteristics were closely maintained during dynamic operation, any necessity for dynamic calibration was eliminated.

4. For optimum accuracy, high torsion-shaft working stress should be employed, the torquemeter installation should be such as to eliminate axial stresses, and an accurate measurement of operating torsion-shaft temperature should be made.

Flight Propulsion Research Laboratory,
National Advisory Committee for Aeronautics,
Cleveland, Ohio, July 26, 1949.

REFERENCES

1. Ruge, Arthur C.: The Bonded Wire Gage Torquemeter. Proc. Soc. Experimental Stress Analysis, vol. I, no. 2, 1943, pp. 68-72. (Paper presented before joint meeting S.E.S.A. and A.S.M.E. (New York), Dec. 2-4, 1943.)

2. Warshawsky, Isidore: A Multiple Bridge for Elimination of Contact-Resistance Errors in Resistance Strain-Gage Measurements. NACA TN 1031, 1946.

3. Sutherland, William: A Kinetic Theory of Solids with an Experimental Introduction. Phil. Mag. and Jour. Sci., vol. 32, no. CXCIV, ser. 5, July 1891, pp. 31-43.

4. Jasper, T. M.: The Value of the Energy Relation in the Testing of Ferrous Metals at Varying Ranges of Stress and at Intermediate and High Temperatures. Phil. Mag. and Jour. Sci., vol. 46, no. CCLXXIV, ser. 6, Oct. 1923, pp. 609-627.

5. Keulegan, G. H., and Houseman, M. R.: Temperature Coefficient of the Moduli of Metals and Alloys Used as Elastic Elements. Bur. Standards Jour. Res., vol. 10, no. 3, March 1933, pp. 289-320.

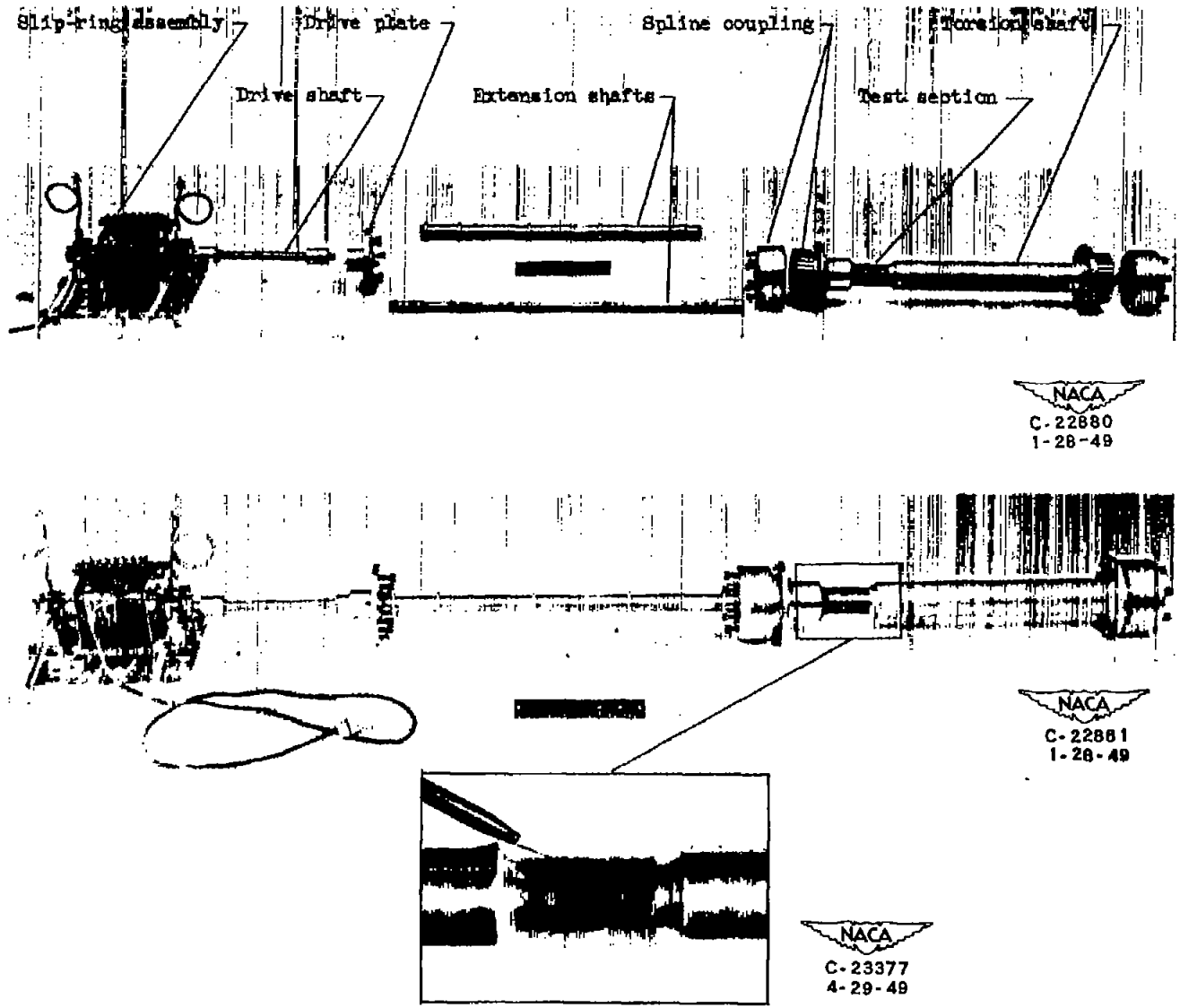

Figure 1. - Strain-gage torquemeter assembly.

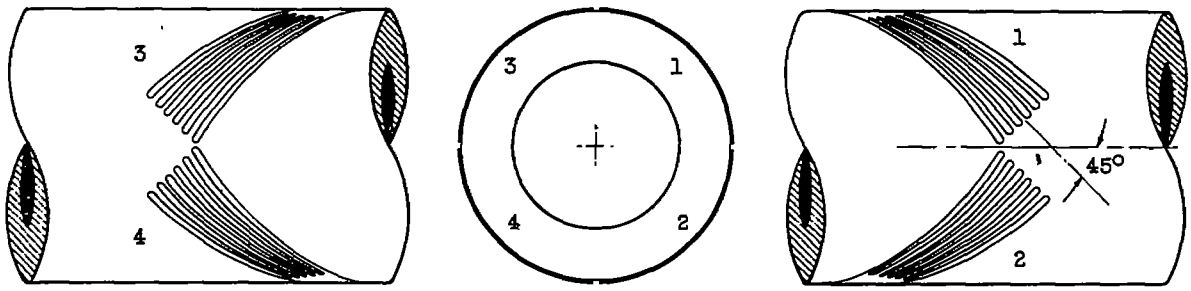

Torsion-shaft test section

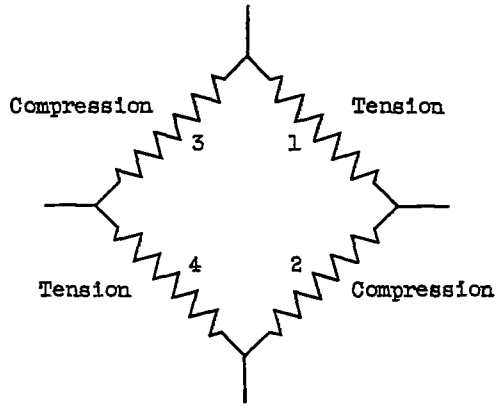

Strain-gage bridge

Figure 2. - Orientation of strain gages on torsion-shaft test section. Advance wire strain gages 1,2,3, and 4 are 350 ohms.

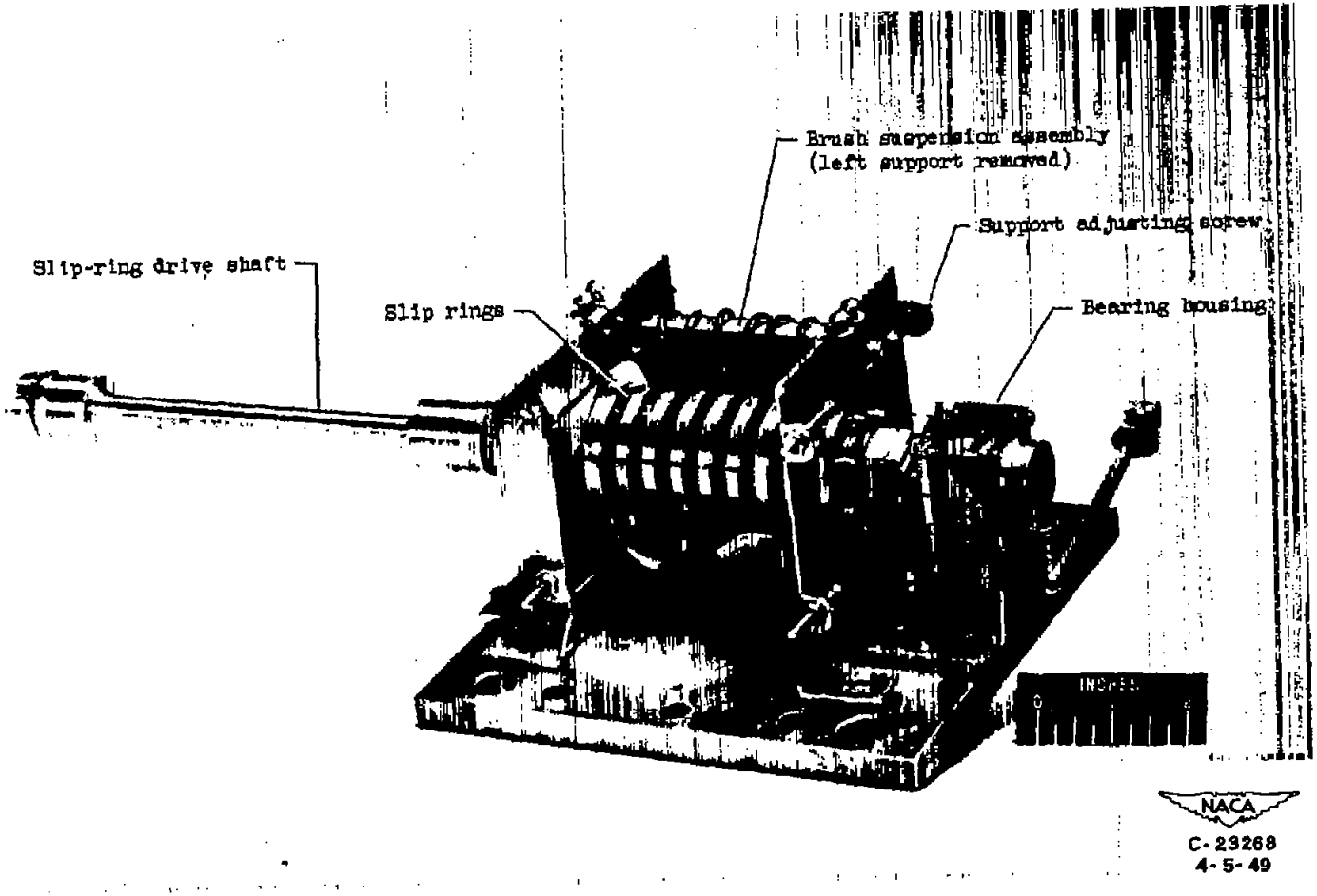

Figure 3. - Slip-ring assembly.

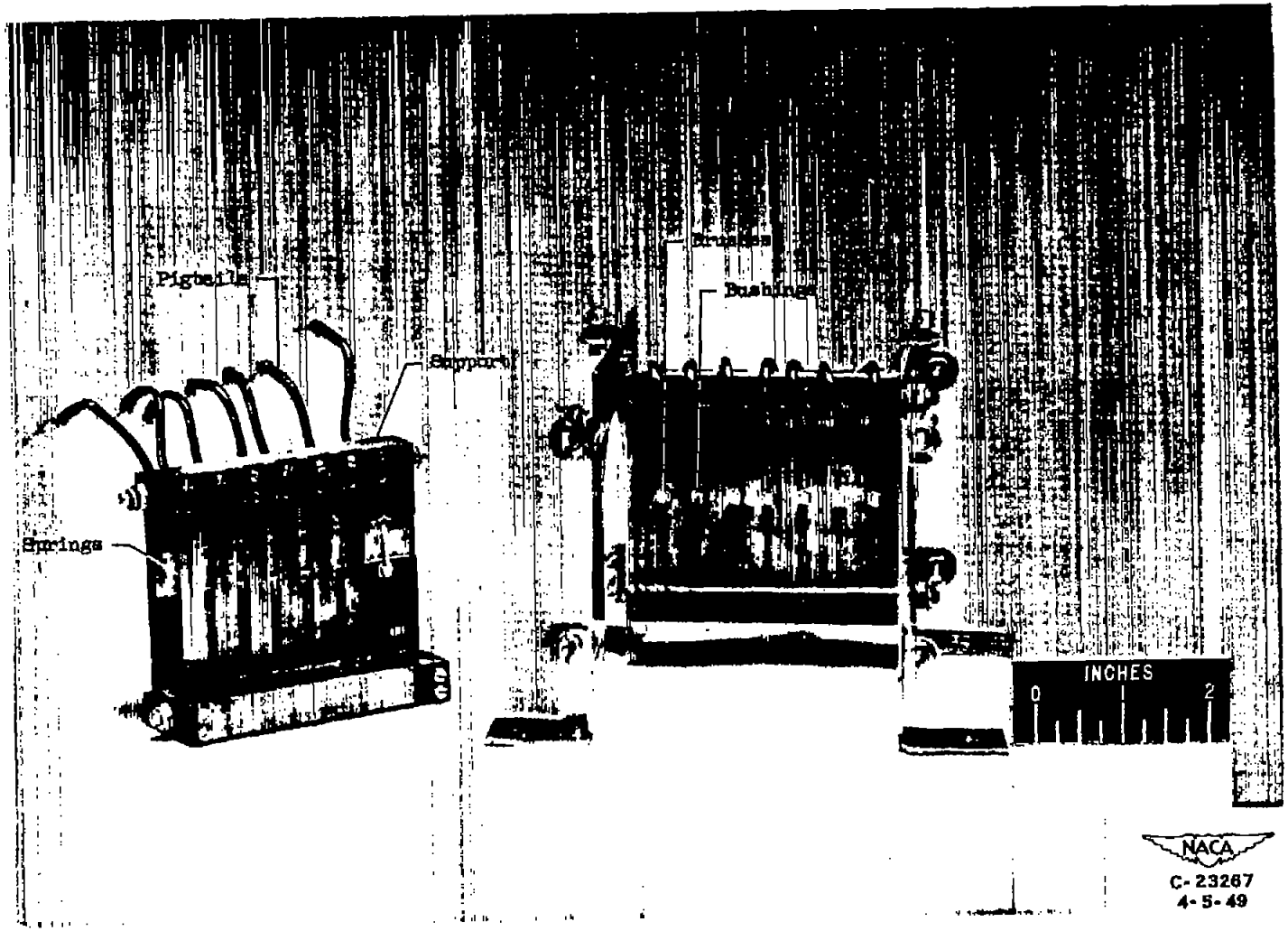

Figure 4. - Brush-suspension assembly.

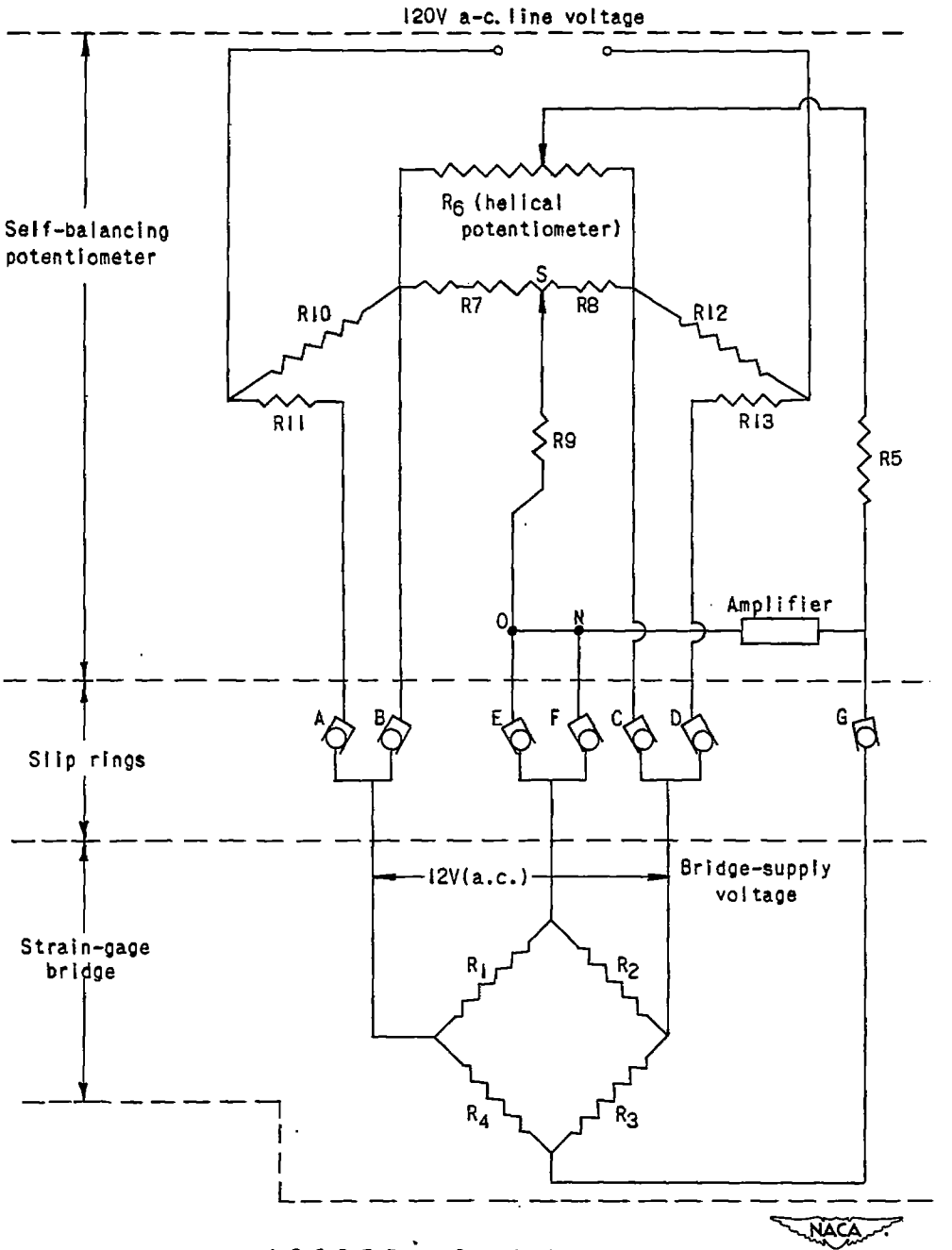

A,B,C,D,E,F, and G	Individual slip rings
R_1,R_2,R_3, and R_4	350-ohm strain gages
R_5 and R_6	Zero adjustment
R_7,R_8, and R_9	Range adjustment
$R_{10} = R_{12}$ $R_{11} = R_{13}$	Resistances minimize effects of contact resistance
S	Slide-wire

Figure 5. - Bridge circuit employed in the strain-gage torquemeter. (Improved operation is obtained when connection between O and N is removed.)

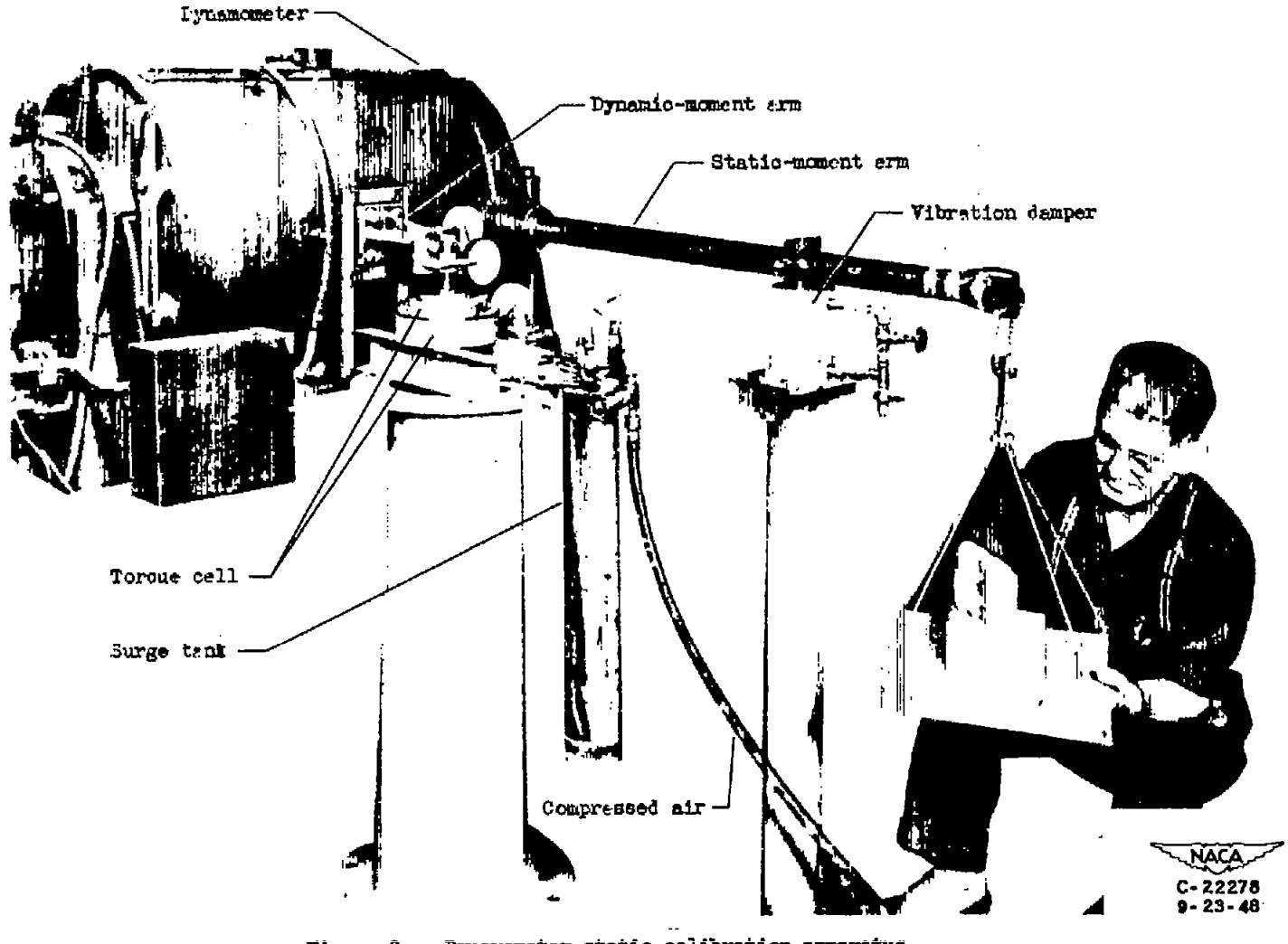

Figure 6. - Dynamometer static-calibration apparatus.

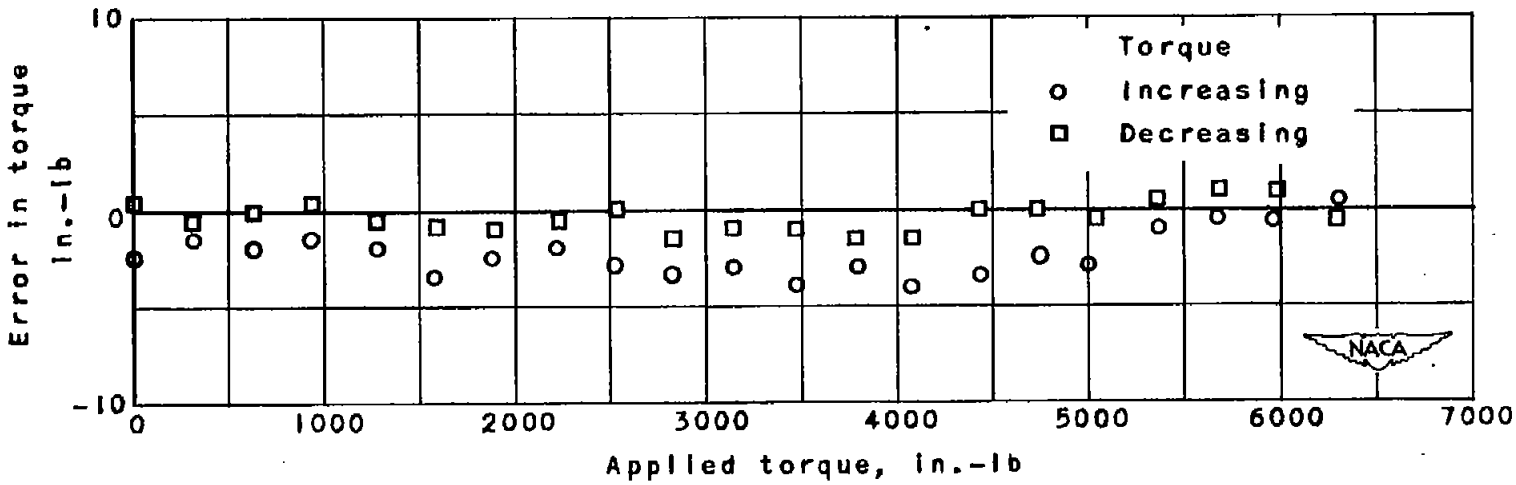

Figure 7. - Results of typical dynamometer static calibration.

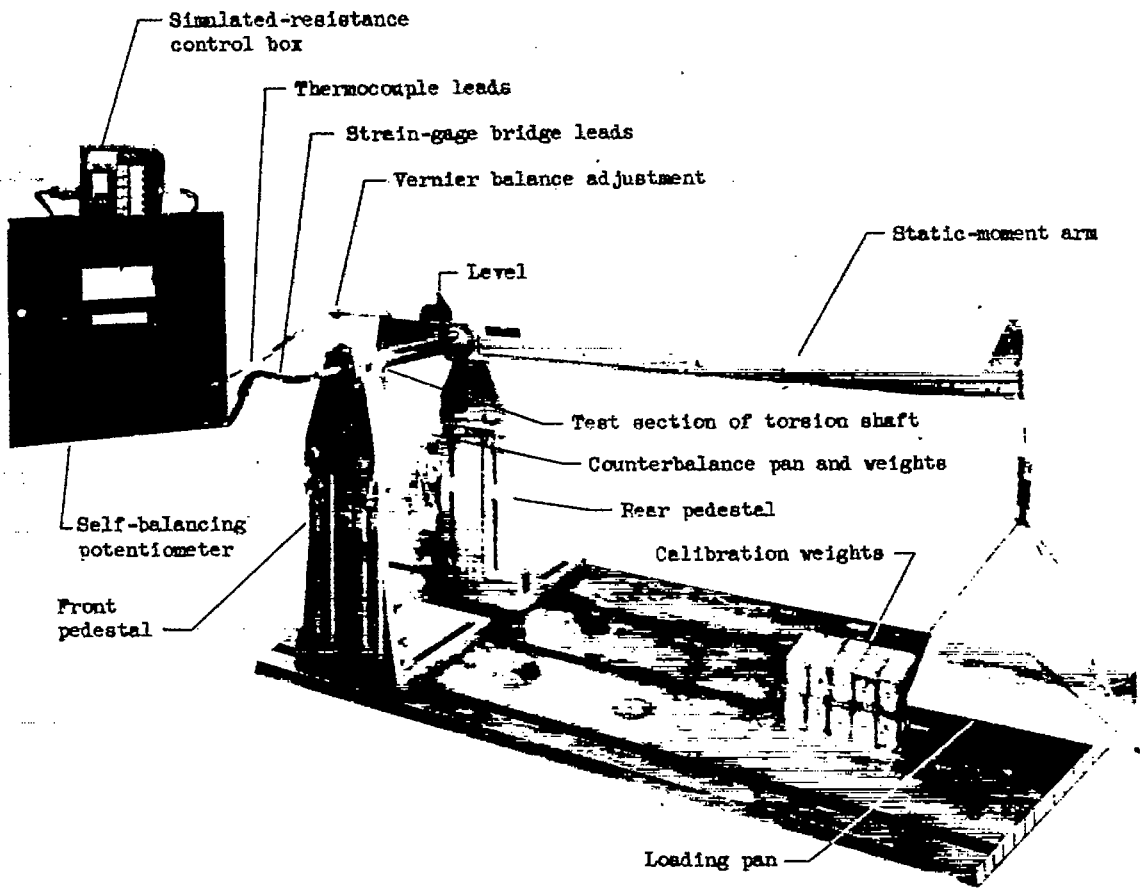

Figure 8. - Torsion-shaft apparatus for static calibration.

NACA
C-23269
4-5-49

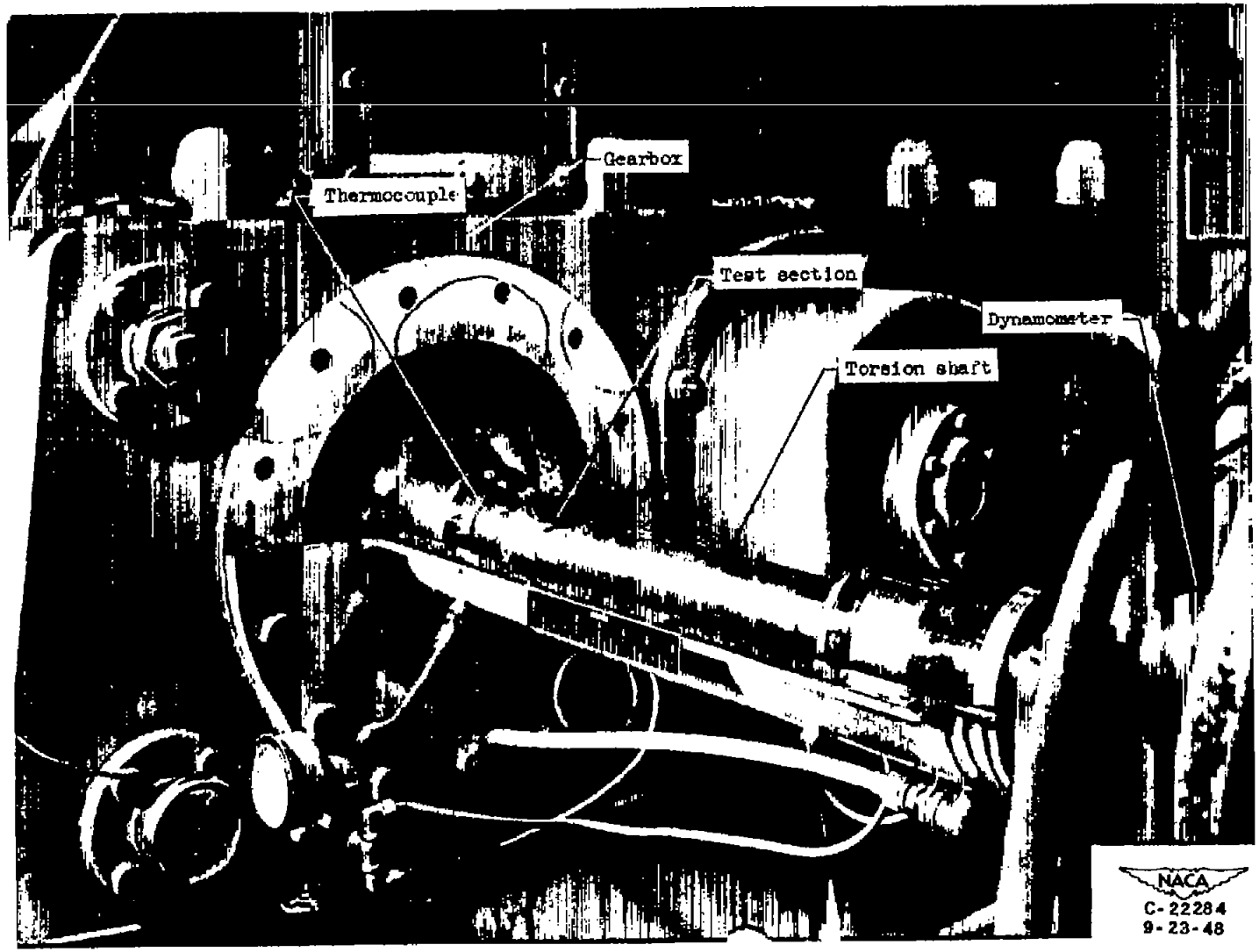

(a) Torsion shaft.

Figure 9. - Installation for dynamic runs.

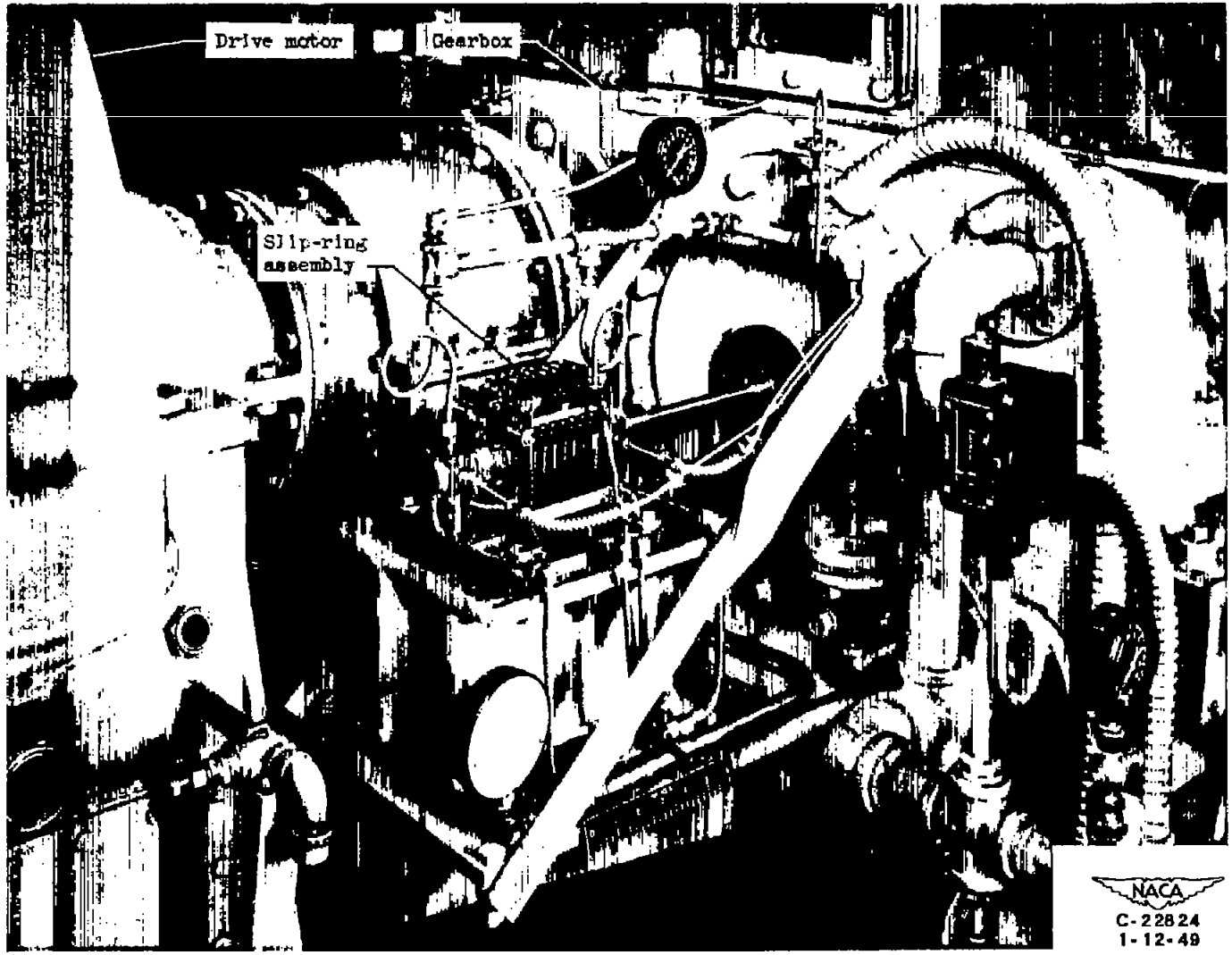

(b) Slip-ring assembly.

Figure 9. - Concluded. Installation for dynamic runs.

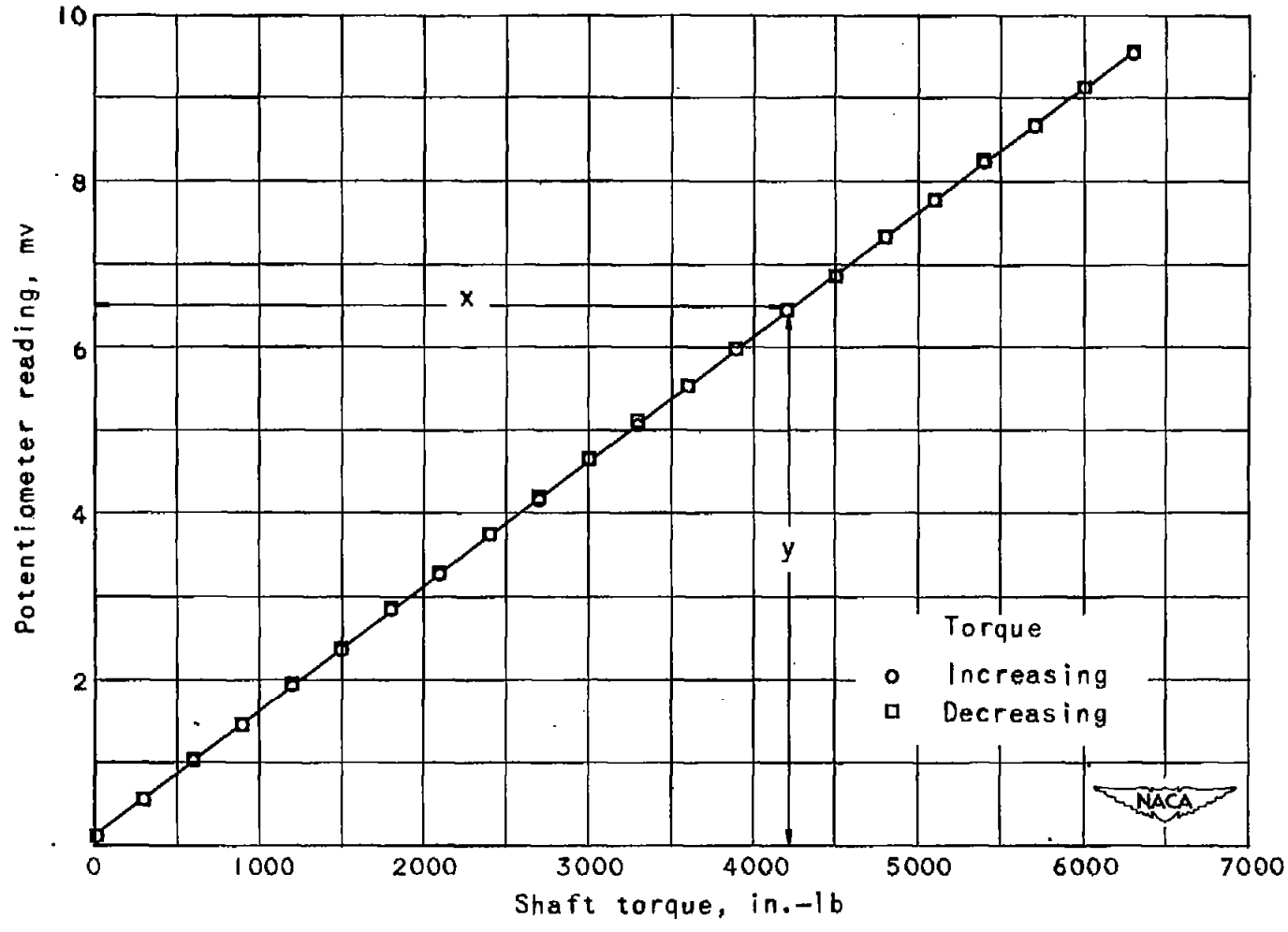

Figure 10.- Static calibration of strain-gage torquemeter (torsion-shaft temperature, 73° F) when contact resistance is present in circuit. Equation for this calibration is $y = (150.37 \times 10^{-5})x + 0.123$.

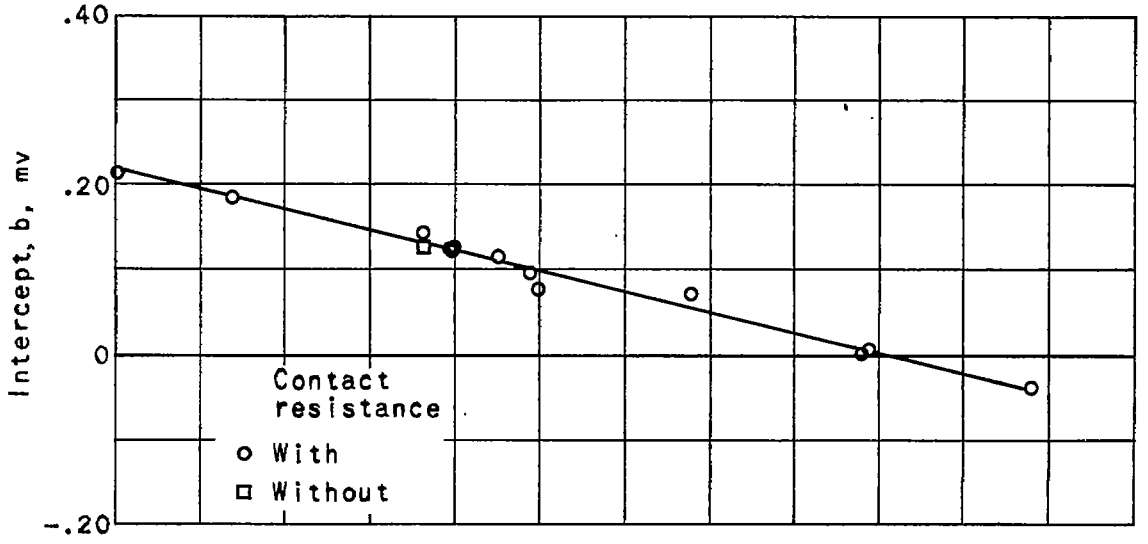

(a) Intercept variation with temperature.

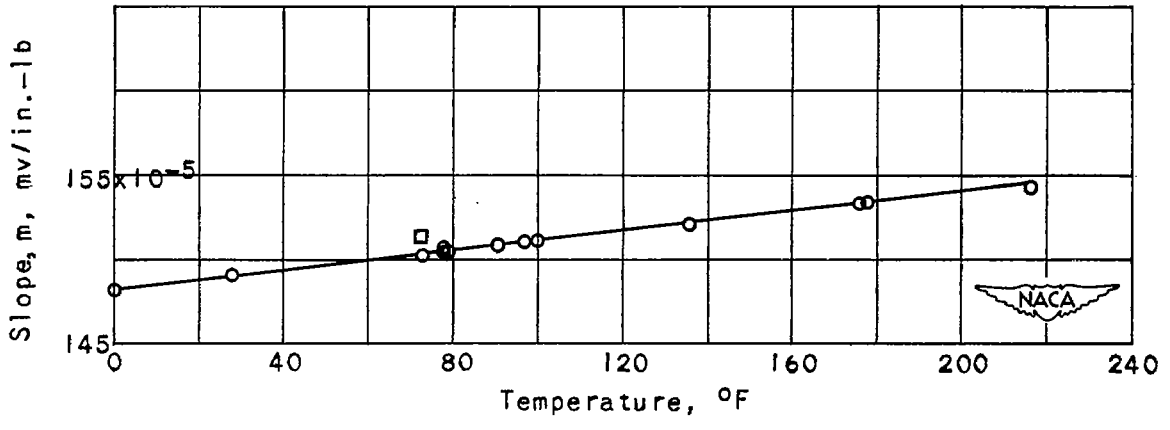

(b) Slope variation with temperature.

Figure 11. – Variation of slope and intercept of static-calibration equations with torquemeter torsion-shaft temperature.

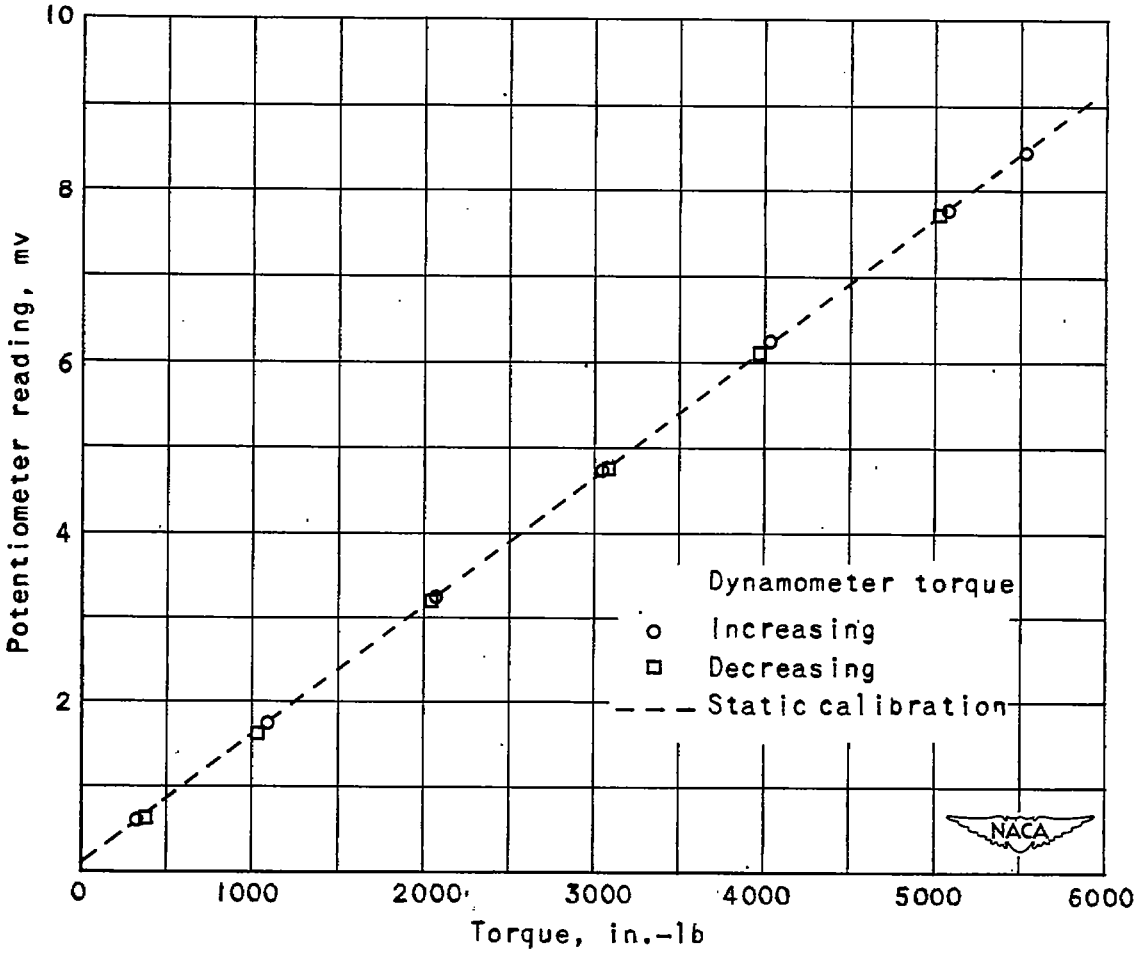

Figure 12. – Comparison of observed dynamic data with static calibration for temperature of 98° F. Observed points for average torsion-shaft temperature at 98° F and shaft speed of 10,000 rpm.

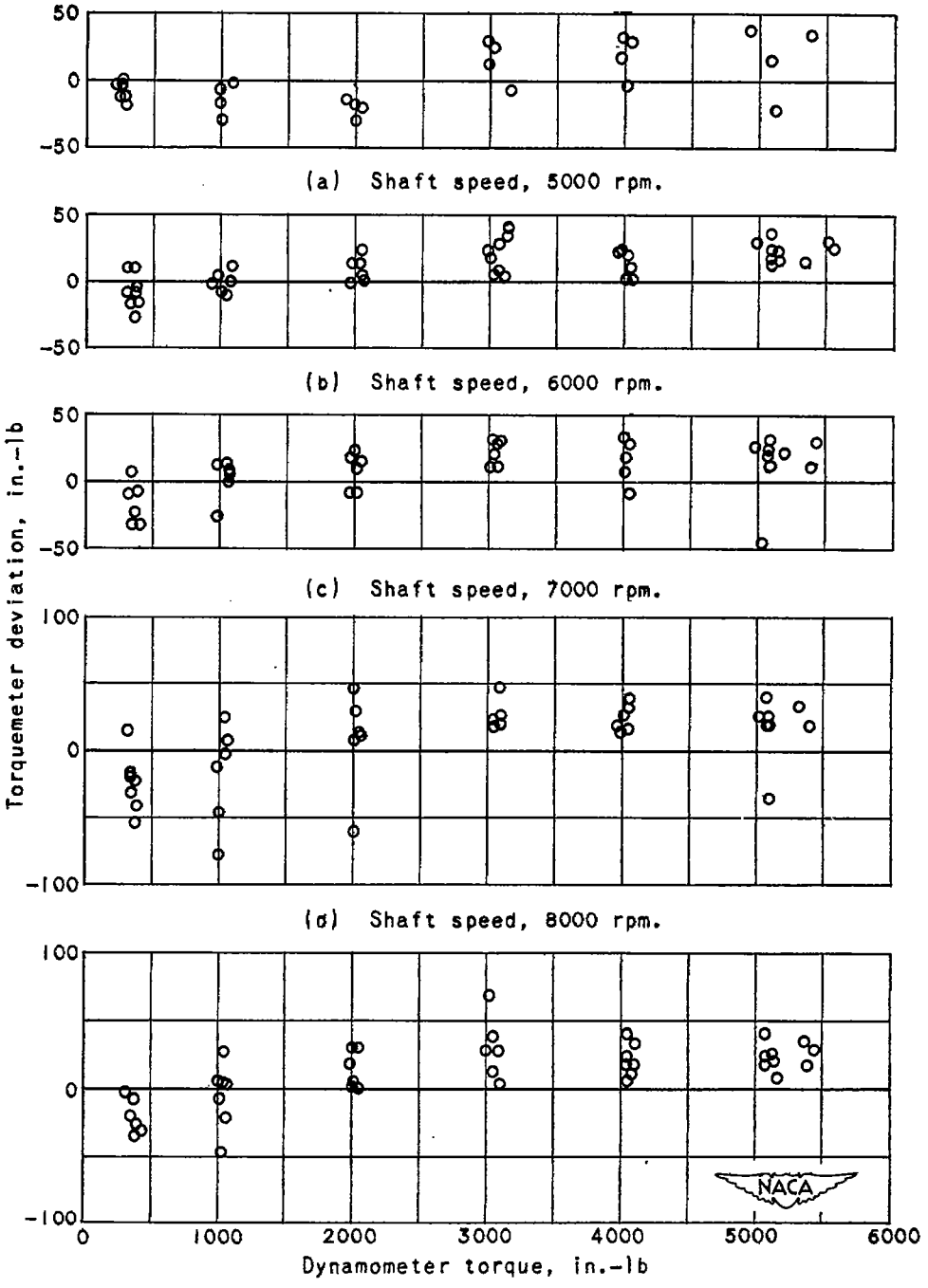

Figure 13. - Variation of torquemeter deviation for range of torque and shaft speed.

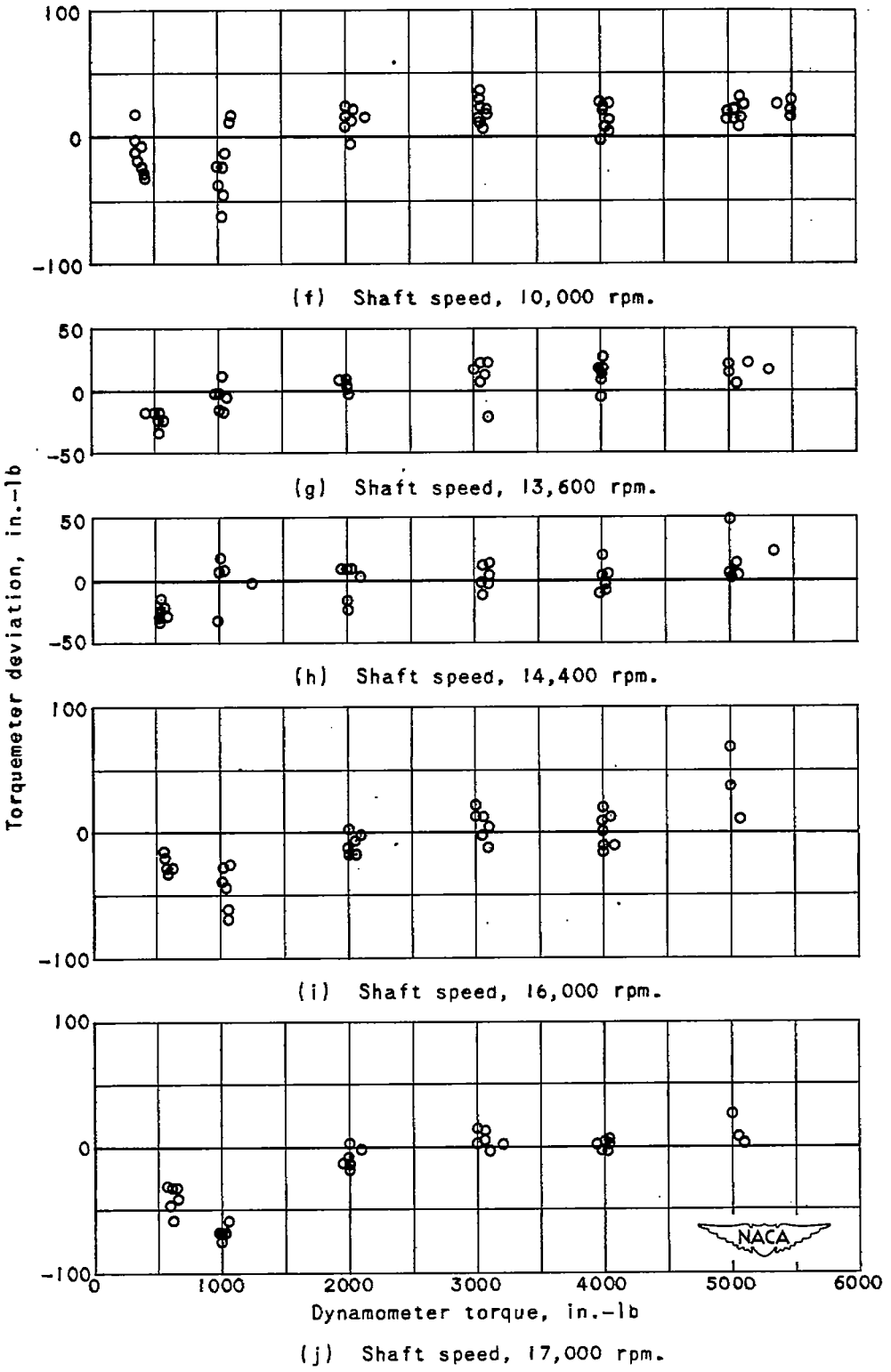

Figure 13. - Concluded. Variation of torquemeter deviation for range of torque and shaft speed.

NACA-Langley - 1-17-50 - 1050